

Greedy optimization for growing stable power grids

Damien Beecroft,^{1,*} Juan G. Restrepo,^{1,†} and David Angulo-Garcia^{2,‡}

¹*Department of Applied Mathematics, University of Colorado at Boulder, Colorado 80309, USA*

²*Universidad de Cartagena. Instituto de Matemáticas Aplicadas. Grupo de Modelado Computacional - Dinámica y Complejidad de Sistemas. Carrera 6 # 36 - 100, Cartagena de Indias, Bolívar - Colombia.*

The power generation and distribution infrastructure is under pressure to accommodate a growing number of distributed renewable energy sources. Since renewables have many sources of temporal variability, it is important that they be added to the power grid in a way that doesn't threaten its stability. In this paper we propose and explore a greedy algorithm by which nodes are sequentially added to a power grid in order to minimize the cost of the added lines and optimize the linear stability of the growing network. We show that, for appropriate parameters, the stability of the resulting network, measured in terms of the dynamics of small perturbations and the correlation length of the disturbances, can be significantly improved with a minimal added line cost. In addition, we analyze numerically the topological properties of the resulting networks and find that, while being more stable, their degree distribution is approximately exponential and independent of the algorithm parameters. Moreover, we find that other topological parameters related with network resilience and efficiency are also affected by the proposed algorithm. Our results are a first step in the development of algorithms for the directed growth of power grids with desirable stability, dynamical and topological properties.

I. INTRODUCTION

The power generation and transmission network is on the brink of a fundamental transformation as renewable sources become a significant fraction of the energy supply [1]. As opposed to the traditional structure in which relatively few and large power plants supply most of the energy, the current trend is to increasingly rely on a larger number of renewables including wind, solar, and geothermal [2]. While the output of large power plants can be controlled to match demand and guarantee the stable operation of the power grid, the output of renewable energy sources is subject to fluctuations caused by environmental conditions, posing challenges to the stability of the power grid [2]. Even though analytical and computational methods to calculate the regions of stability in power systems have been developed for decades [3–5], it is only recently that this problem has been tackled from the dynamical network theory perspective. This new approach has shed light on the impact of several factors that affect the linear and nonlinear stability of a power grid [6–12].

Since it is expected that power grids will continue to grow by the addition of numerous renewable energy sources, it is of interest to study how their properties might be tailored by a judicious choice in how new nodes are added. Previous works have considered the growth of power grids by optimizing the addition of new nodes to optimize properties of the resulting network such as redundancy [13], robustness to removal of nodes and path length [14], and other topological features such as vari-

ability in betweenness centrality and clustering coefficient (for more details see [15]). Instead of focusing on topological properties of the growing networks, we propose a greedy algorithm that directly optimizes the dynamical properties of the network. More precisely, our algorithm optimizes a combination of the cost of the grid (taken to be proportional to the total line length) and a measure determinant of linear stability (a similar algorithm has been proposed for the growth of the internet [16]). Remarkably, we find that by using our algorithm the stability of the grown power grids can be significantly improved without an appreciable increase in line length. While our greedy algorithm is not optimal, we expect it will pave the way to the development of more sophisticated algorithms.

Our paper is organized as follows. In Sec. II A we present our model for the growing power grid and the optimization algorithm. In Sec. III we analyze the topological and dynamical properties of the power grids obtained from the growing algorithm. Finally, we discuss our results and present our conclusion in Sec. IV.

II. MODEL AND METHODS

A. Power Grid Model

We start by considering a second order Kuramoto model which describes, in a simplified way, the behavior of a Power Grid [17]. We consider a coarse grained description of the power grid in terms of N nodes which represent generators and consumers. The state of each node can be represented by its phase angle ϕ_i and its angular velocity $d\phi_i/dt$. For the power grid to operate correctly, nodes must synchronize at the nominal frequency $\Omega = 2\pi f$ (where f is either 50 Hz or 60 Hz), and synchronization can be studied analyzing the phase deviation of

*Electronic address: damien.beecroft@colorado.edu

†Electronic address: juanga@colorado.edu

‡Electronic address: dangulog@unicartagena.edu.co

node i with respect to the reference phase Ωt , namely $\theta_i(t) = \phi_i(t) - \Omega t$. In this comoving reference frame the dynamics of θ_i and its velocity $\dot{\theta}_i$ can be described by the second-order Kuramoto model:

$$\ddot{\theta}_i(t) = P_i - \alpha_i \dot{\theta}_i(t) + \sum_j^N \mathcal{K}_{ij} \sin[\theta_j(t) - \theta_i(t)]. \quad (1)$$

Here P_i is the injected power at node i (up to a scaling factor) and it is positive (negative) for generators (consumers). The parameter α_i quantifies the damping coefficient of node i , and \mathcal{K}_{ij} is the maximum power transfer capacity from node i to node j , which depends on the impedance of transmission lines connecting them. For a derivation and details of the model the reader is referred to [18, 19]. For simplicity, we will assume that $\mathcal{K}_{ij} = K A_{ij}$, where K is constant and A_{ij} are the entries of an $N \times N$ unweighted, symmetric adjacency matrix A .

In the comoving reference frame, synchronization of (1) can be assessed calculating the stability of the fixed point $\dot{\theta}_i = 0$, $\theta_i = \theta_i^*$, where the fixed point phases θ_i^* satisfy the equation

$$0 = P_i + K \sum_j^N A_{ij} \sin(\theta_j^* - \theta_i^*). \quad (2)$$

For small angle differences, the equilibrium can be approximated by

$$\boldsymbol{\theta}^* \approx \frac{1}{K} \mathcal{L}^\dagger \mathbf{P} \quad (3)$$

where \mathcal{L}^\dagger is the pseudo-inverse of the Laplacian matrix $\mathcal{L} = \text{diag}(\sum_{j=1}^n A_{ij}) - A$, $\boldsymbol{\theta} = [\theta_1^*, \theta_2^*, \dots, \theta_N^*]^T$, and $\mathbf{P} = [P_1, P_2, \dots, P_N]^T$.

The stability of the synchronized solution $\dot{\theta}_i = 0$, $\theta_i = \theta_i^*$ is determined by linearization of Eq. (1). While a simple, closed-form condition for linear stability valid in general is not available, it has been shown in [6] that for a large class of network topologies a stable synchronized state with cohesive phases $|\theta_i^* - \theta_j^*| \leq \gamma < \pi/2$ can be achieved when

$$\Delta \equiv \frac{1}{K} \|B^T \mathcal{L}^\dagger \mathbf{P}\|_\infty < \sin(\gamma), \quad (4)$$

where B is the directed incidence matrix. Note that, taking the limit $\gamma \rightarrow \pi/2$ and recalling the small phase difference approximation of the equilibrium in Eq. (3), Equation (4) can be interpreted as saying that, in order to achieve stable synchronization, the worst (largest) difference between the steady phase of connected pairs in the network has to be lower than the coupling strength K [6]. The variable Δ is then a useful indicator when designing power grid networks, as it is an easily calculated index of stability. A lower Δ is an indication of a more *linearly* stable power network [20].

A natural question is whether a network can be optimized to maximize linear stability of the synchronized

state (i.e., minimize Δ) while keeping the costs of adding lines low. To address this question, we propose a network growth model where nodes are added sequentially to a network and, each time a node is added, a combination of line cost and Δ is minimized by using a greedy algorithm.

B. Power Grid growing algorithm

As distributed generation of energy using renewable sourced increases, it is expected that a large number of nodes will be added to existing power grid in a decentralized manner. When a new node is connected to the power grid, a natural choice is to connect it to the closest nodes so as to minimize the added line length. However, here we propose that by connecting the new node to other nearby nodes, one can improve the stability of the power grid without significantly increasing the line length. While there have been models for growing power grids that optimize network metrics such as robustness to node removal, assortativity, path length, and others [15, 21], our model specifically addresses the optimization of a quantity that directly influences dynamical stability. We propose the following recursive power grid growth model:

1. At time $t = 0$, the algorithm is initialized with a seed network of size n_0 spatially embedded in a simply connected region $M \subseteq \mathcal{R}^2$, and connected via their minimum spanning tree. Each node i is characterized by coordinates $(x_i, y_i) \in M$ and an associated power P_i chosen in such a way that $\sum_{i=1}^{n_0} P_i = 0$.
2. At time $t > 0, t \in \mathbb{N}$, a new node is created with coordinates (x_{n_0+t}, y_{n_0+t}) chosen randomly from a prescribed probability density $f(x, y)$ and with associated power P_{n_0+t} chosen randomly from a uniform distribution in $[-1, 1]$. The power is balanced evenly between the generating nodes, i.e., the powers are updated by

$$P_i \rightarrow \begin{cases} P_i, & P_i \leq 0, \\ P_i - \frac{P_{t+1}}{N_+} \dots P_i > 0, i < n_0 + t, \end{cases} \quad (5)$$

where N_+ is the number of previously existing nodes with positive power (generators).

3. The newly added node establishes r links to existing nodes, where the r nodes are chosen among the closest q nodes to node $t+1$ in such a way that the following cost function is minimized

$$\mathcal{C} = s\Delta + (1-s)L, \quad (6)$$

where L is the total (euclidean) line length after the new node is connected to the other j nodes, Δ is defined in Eq. (4), and $s \in [0, 1]$.

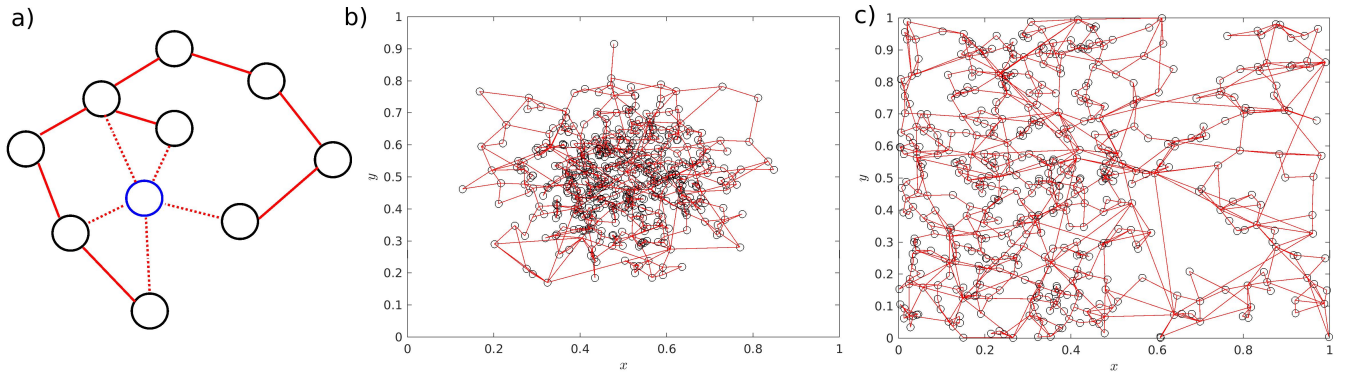


FIG. 1: a) A new node (blue) is placed at a position (x_{t+1}, y_{t+1}) chosen randomly from the distribution $f(x, y)$. Potential connections (dashed lines) to the q closest nodes are evaluated, and the r connections with the lowest cost function \mathcal{C} are established. Networks constructed by following the growing algorithm with added node positions chosen b) with the x and y positions chosen independently from Gaussians centered at 0.5 and with standard deviation $1/8$, and truncated so that the positions remain in $(0, 1)$, and c) the y position is chosen uniformly in $(0, 1)$, and the x coordinate is chosen from a piecewise constant distribution given by $8/5$ for $0 < x < 1/2$, $2/5$ for $1/2 < x < 1$, and 0 otherwise. The other parameters of the algorithm are $s = 0.5$, $q = 5$, and $r = 2$. The initial seed networks have 10 nodes placed uniformly in the square $(0.4, 0.6) \times (0.4, 0.6)$ connected via their minimum spanning tree, and the final networks has 510 nodes.

4. Steps 2 and 3 are repeated until a network of desired size N is produced.

The first term on the right hand side of the cost function [Eq. (6)] controls the degree of influence of the linear stability in the growing algorithm, while the second term controls the cost of establishing lines. A value of $s = 0$ seeks only to minimize the line cost and $s = 1$ seeks to enhance the linear stability of the resulting network. Figure 1(a) illustrates the addition of a new node to the existing network (black circles with solid red lines). The new node (blue circle) is added at a random position, and potential links (dashed lines) to the $q = 5$ closest nodes are evaluated. The r links that minimize \mathcal{C} are established, and the procedure is then repeated with a new node.

Figs. 1(b-c) show two networks constructed by following the previous algorithm. In (b), the x and y positions are chosen independently from a Gaussian distribution centered at 0.5, with standard deviation $1/8$, and truncated so that the positions (x_i, y_i) remain within the region $M = (0, 1) \times (0, 1)$. In (c), the y position is chosen uniformly in $(0, 1)$, and the x coordinate is chosen from a piecewise constant distribution given by $8/5$ for $0 < x < 1/2$, $2/5$ for $1/2 < x < 1$, and 0 otherwise. The other parameters are $s = 0.5$, $q = 5$, and $r = 2$. The seed network consists of 10 nodes placed uniformly in the square $(0.4, 0.6) \times (0.4, 0.6)$ connected via their minimum spanning tree.

III. DYNAMICAL AND TOPOLOGICAL FEATURES OF THE GROWING POWER GRIDS

In this Section we show first how the grid growing algorithm can increase the stability of the grown grids with

a negligible added cost. Then, we study additional dynamical characteristics of the grown grids such as linear stability and the correlation length of perturbations, and topological indicators such as degree distribution, clustering coefficient and betweenness centrality.

A. Reduction of Δ with negligible cost

The basis of the growing algorithm is that, by allowing for connections to more distant nodes, the parameter Δ is reduced at the expense of increasing total line length L . Therefore, we expect that, as s varies, Δ decreases as L increases. This is verified in Figure 2(a), where we plot Δ versus L averaged over 100 realizations as s is varied from 0 to 1 (indicated by the color bar) for $q = 5$. The inset shows the same data for $q = 3$ (black circles), $q = 5$ (blue x's), and $q = 10$ (red +'s). While the plot confirms the above expectations, it also reveals the following behavior:

- Remarkably, for low values of s there is a very sharp and significant decrease in Δ with an almost negligible increase in line length L .
- For a *fixed* line length L , Δ decreases with increasing q .

The first observation can be understood heuristically by considering the situation where a new node is added, and two potential connections are considered to nodes i and j . If node i is much more beneficial to minimize Δ than node j , but its distance to the new node is slightly larger than that of node j , a small but positive value of s allows for the selection of node i while only slightly increasing L . To understand the second observation, one can imagine all the possible ways in which a total line length L

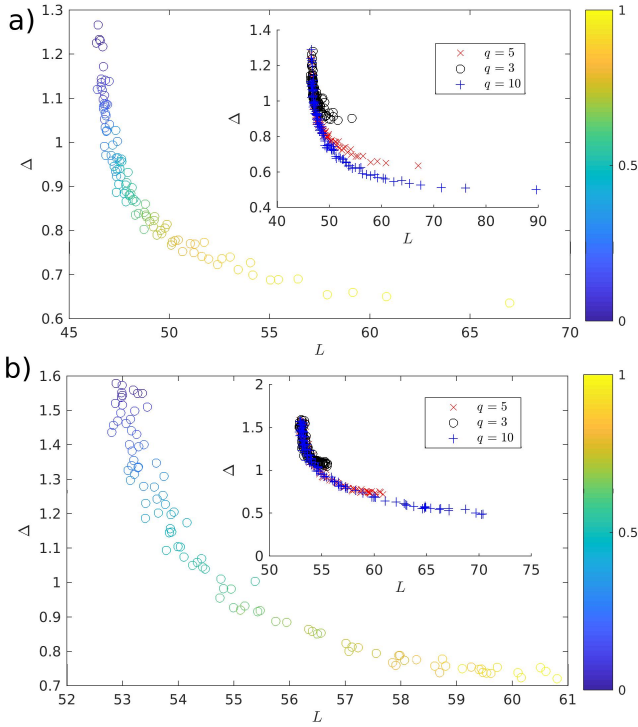


FIG. 2: a) Stability parameter Δ versus total line length L averaged over 100 realizations for $q = 5$, $r = 2$. The parameter s is varied from 0 to 1 as indicated in the color bar. The inset shows the same results for $q = 3$ (black circles), $q = 5$ (blue x's), and $q = 10$ (red +s). b) Results from the toy model described in the Appendix showing similar qualitative results

is achieved. Since those with higher q are obtained by allowing more potential connections, they allow for more chances to minimize Δ and should result therefore, on average, on a lower value of Δ .

The above heuristic arguments are based solely on local considerations, and ignore the full complexity of how Δ depends on the network and the node parameters. To show that such local considerations can, indeed, result in the observed behavior, we considered a toy model where nodes are added sequentially, and the distances to and phase differences from potential connections are sampled from appropriate distributions (see Appendix for details). This stochastic model reproduces qualitatively the numerical results as shown in Fig. 2(b).

In summary, although the growing algorithm is based on the competition between line length and stability, the results in Fig. 2 show that one can improve stability without increasing the line length by (i) using small values of s , or (ii) increasing q and adjusting s appropriately.

B. Reduction of critical coupling constant

The growing algorithm is designed to minimize Δ , which is a convenient indicator of linear stability. To study how the linear stability of the grown grids is actually improved, we perform the following numerical experiment: first we set K at value high enough that the grown networks have linearly stable fixed points for all s in $(0, 1)$ (we used $K = 7$). For a given value of s , we grow a power grid of $N = 100$ nodes. Solving numerically Eq. (1), the phases θ_i settle at their fixed point values θ_i^* . Then, we adiabatically decrease K until, at some value $K = K_c$, the system loses stability. The value of K_c is averaged over 100 realizations and the process is repeated for different values of s . The critical coupling strength K_c is plotted versus s in Fig. 3(a) for $q = 5$ and $r = 2$ (black circles), 3 (red x's), and 4 (blue diamonds). For $r = 2$ there is a significant reduction in the critical coupling as s is increased, corresponding to a more linearly stable system. For $r = 3$ and $r = 4$, K_c is smaller since there are more connections overall, but the reduction in K_c as s is increased is not as significant because the options when connecting a new node are reduced. Complementing the results shown in Fig. 2, we see that by increasing s from 0 to 0.85 for $r = 2$, K_c is decreased by approximately 40% while the line length, shown in Fig. 3(b), increases only by about 10%.

C. Linear stability

Now we study the linear stability properties of the grids grown using our algorithm. While we have shown that higher values of s reduce the critical coupling K_c at which the fixed point θ^* becomes linearly unstable, here we show that, on the other hand, for high enough values of K the linear stability properties of the grown networks are largely independent of s .

Introducing the variable $\omega_i \equiv \dot{\theta}_i$, the linearization around the equilibrium $\omega_i^* = 0$ and θ_i^* given by Eq. (3) of the system (1) results in

$$\delta \dot{\theta}_i = \delta \omega_i, \quad (7)$$

$$\delta \dot{\omega}_i = -\alpha \delta \omega_i - K \sum_{j=1}^N \mathcal{L}(\theta^*)_{ij} \delta \theta_j, \quad (8)$$

where

$$\mathcal{L}(\theta^*)_{ij} = \begin{cases} -A_{ij} \cos(\theta_j^* - \theta_i^*), & i \neq j, \\ -\sum_{k \neq i}^N L_{ik}, & i = j, \end{cases}$$

are the entries of the so-called state-dependent Laplacian matrix $\mathcal{L}(\theta^*)$ [21]. This shorthand notation allows us to write the Jacobian matrix of the system as

$$J = \begin{bmatrix} -\alpha I & -K \mathcal{L}(\theta^*) \\ I & \mathbf{0} \end{bmatrix}, \quad (9)$$

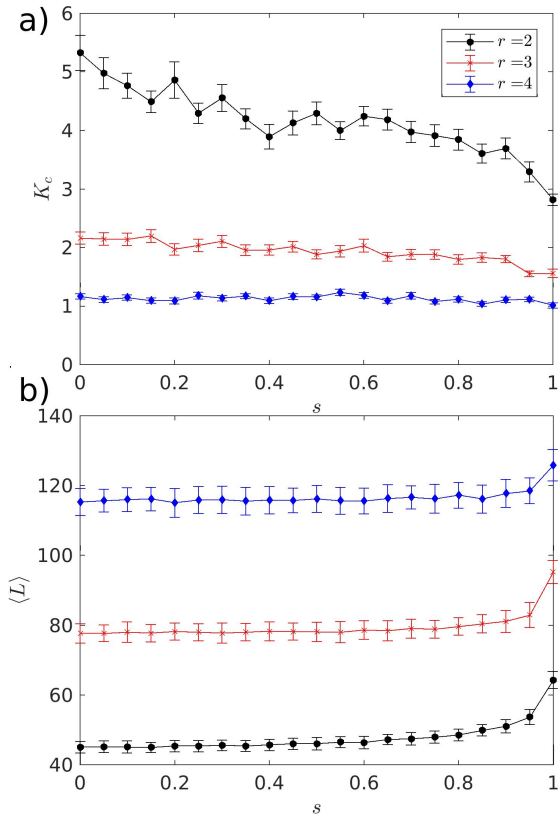


FIG. 3: a) The value of K at which the synchronized fixed point loses stability, K_c , and b) the total line length L as a function of s for $r = 2$ (black circles), $r = 3$ (red x's), and $r = 4$ (blue diamonds). The symbols show an average over 100 realizations and the bars represent one standard deviation.

where I is the $N \times N$ identity matrix. With this formulation, the eigenvalues of the Jacobian matrix can be expressed as

$$\mu_i = -\frac{\alpha}{2} \pm \frac{1}{2} \sqrt{\alpha^2 - 4K\lambda_i(\mathcal{L}(\theta^*))}, \quad (10)$$

where $\lambda_i(\mathcal{L}(\theta^*))$ is the i th eigenvalue of $\mathcal{L}(\theta^*)$. Whether or not an eigenvalue μ_i has positive real part is determined by whether the eigenvalues $\lambda_i(\mathcal{L}(\theta^*))$ are all positive or not. When $A_{ij}|\theta_i^* - \theta_j^*| < \pi/2$ for all connected i, j , $\mathcal{L}(\theta^*)$ is diagonally dominated and positive semidefinite. In that case, since the value α is in general small to account for the damped oscillatory behavior of perturbations in the grid, all the eigenvalues μ_i have the same negative real part, $-\alpha/2$. The condition $A_{ij}|\theta_i^* - \theta_j^*| < \pi/2$ for all connected nodes i, j is obtained when $\Delta \equiv \frac{1}{K} \|B^T \mathcal{L}^\dagger \mathbf{P}\|_\infty < 1$. Since B , \mathcal{L}^\dagger , and \mathbf{P} are independent of K , for large enough K the fixed point θ^* is linearly stable, with Jacobian eigenvalues with identical and negative real part. To test this prediction, we generate networks at varying values of s and fixed K . For each network, we perturb the nodal variables $\mathbf{x} = (\theta, \omega)$ from the synchronized fixed point \mathbf{x}_p and plot in Fig. 4(a) the logarithm of the euclidean distance

between the perturbed trajectory and the fixed point, $\|\mathbf{x} - \mathbf{x}_p\|$ as a function of time for all networks. From linearization one would expect that the distance evolves as $\|\mathbf{x} - \mathbf{x}_p\| \propto \exp(\mu t)$, where μ is the leading eigenvalue of the Jacobian. As seen in the Fig. 4(a), the decay rate of the perturbations is independent of s and approximately equal to $-\alpha/2$ (see magenta line with slope $-\alpha/2$). This is not surprising as the real part of the eigenvalues is associated with the decay rate of the perturbations and this value is independent of s as mentioned before. Interestingly, we also find that the frequency response of the perturbations, seen in the frequency spectrum [Fig. 4(b)] and the distribution of the imaginary part of the eigenvalues [Fig. 4(c)] is also largely independent of s . Thus, for large K , the linear response of the system does not depend on s . For moderate values of K , however, as shown in Fig. 3(a) and discussed earlier, the value of s can be determinant for the linear stability of the fixed point.

D. Correlation length function

With the aim of further assessing the level of network resilience, we calculated the correlation length function of small (but finite) perturbations. Given a perturbation at a given node, the correlation length function $\xi(d)$ is defined as the average correlation between the phase dynamics of every pair of nodes (i, j) in the network at a topological distance $D_{ij} = d$. The topological distance for every pair of nodes in the network, in turn, is calculated as the length of the shortest path between them. Altogether, the correlation length function reads as

$$\xi(d) = \frac{1}{N_d} \sum_{(i,j):D_{ij}=d} \left(\frac{\sum_t (\theta_i(t) - \bar{\theta}_i)(\theta_j(t) - \bar{\theta}_j)}{\sqrt{\sum_t (\theta_i(t) - \bar{\theta}_i)^2 (\theta_j(t) - \bar{\theta}_j)^2}} \right). \quad (11)$$

Here N_d is the number of pairs of nodes at a given distance d and $\bar{\theta}_i$ is the time average of the phase $\theta_i(t)$. It is useful to calculate the first zero crossing of the correlation function (ξ_0) and use this as an indicator of how far the effect of a perturbation propagates through the network.

In Fig. 5(a) we report $\xi(d)$ for $s = 0$ (blue line) and $s = 1$ (red line). For this test, we have assumed a connection strength $K = 2$ to guarantee consistent degrees of synchronization. From this panel it is possible to see how networks generated via a transmission-line-length optimization criteria ($s = 0$) have a larger value of correlation length $\xi_0 \approx 4$, in contrast to networks generated following line load minimization algorithm ($s = 1$), which give $\xi_0 \approx 3$. This trend was consistent across all the values of $s \in [0, 1]$ for $r = 2$ and $r = 3$, where a linear decrease of ξ_0 was found at increasing s (see Fig. 5(b)). However, at $r = 4$ there is virtually no difference between the correlation length at $s = 0$ and $s = 1$. To better understand

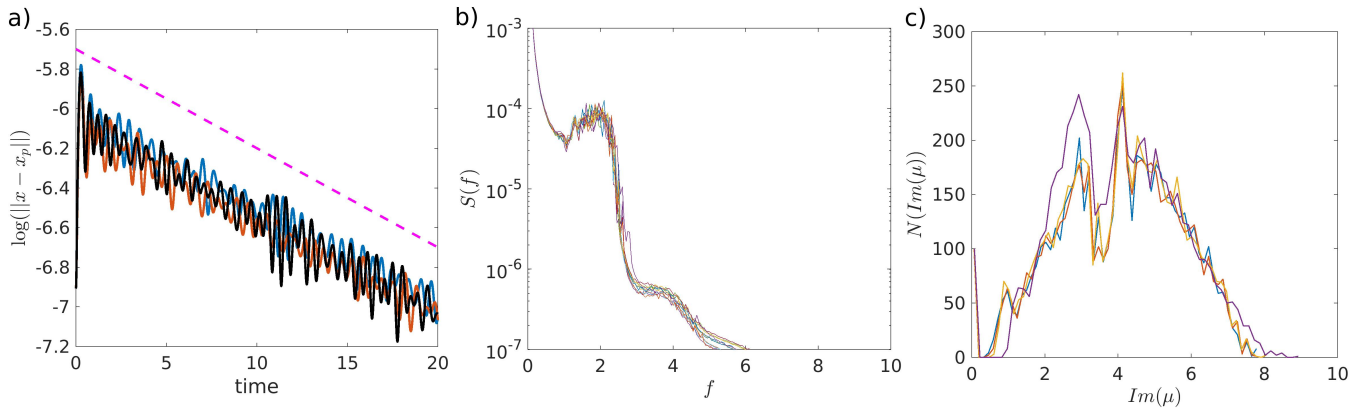


FIG. 4: a) Logarithm of the distance between the fixed point \mathbf{x}_p and the perturbed trajectory \mathbf{x} as a function of time. Blue, red and black curves correspond to three sample trajectories of networks generated with $s = 0$, $s = 0.5$ and $s = 1$, respectively. The magenta line corresponds to a straight line with slope equals to $-\alpha/2$ showing that the decay rate of the perturbed trajectories towards the fixed point follow an exponential decay with rate $-\alpha/2$. b) Frequency spectrum of the perturbations \mathbf{x}_p for various values of s . c) Histogram of the imaginary part of the eigenvalues (10) of the state-dependent Laplacian for various values of s .

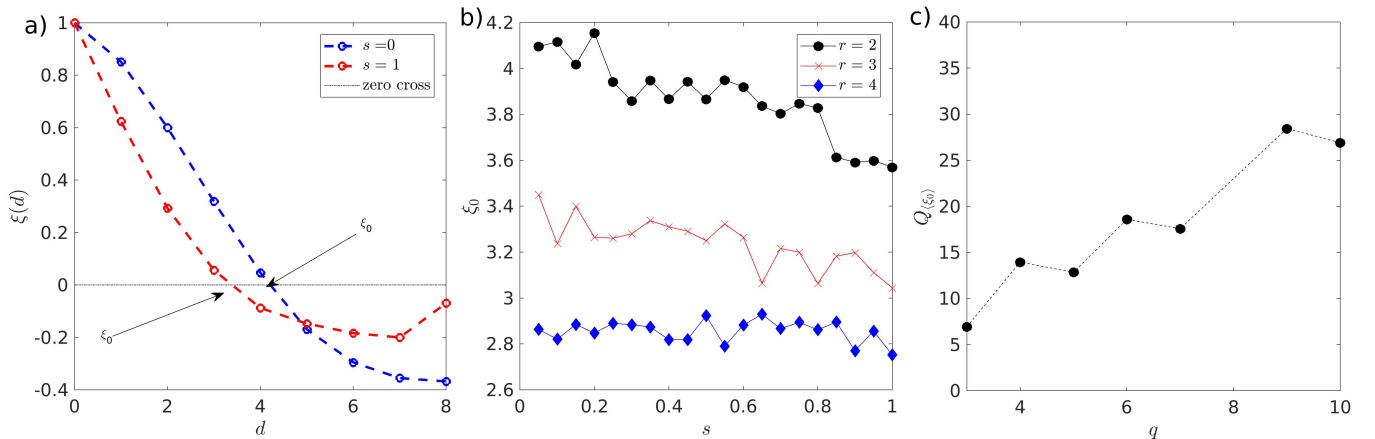


FIG. 5: a) Sample correlation length function for $s = 1$ (red) and $s = 0$ (blue) indicating the first-zero crossing. b) First zero crossing of the correlation length function as a function of s (symbols) for $K = 2$ at three different values of r indicated in the legend of the figure. c) Relative change between $s = 0$ and $s = 1$ for different values of q at a fixed value of r . We used $N_{seed} = 6$, $N = 94$, $q = 5$. We used $r = 2$ in panels (a) and (c). The correlation length function is calculated averaging 20 iterations for each s .

the trend of ξ_0 at varying values of q , we introduced the relative change of an indicator x between its $s = 0$ value and the $s = 1$ value, namely:

$$Q_{\langle x \rangle} = \frac{\langle x \rangle_{s=0} - \langle x \rangle_{s=1}}{\langle x \rangle_{s=0}} \times 100\% \quad (12)$$

In this equation, and in the following, $\langle x \rangle$ represents the average across realizations of x . In the case of the correlation length $x \equiv \xi_0$ the result of this indicator is depicted in Fig. 5(c) where $Q_{\langle \xi_0 \rangle}$ increases from 5% ($q = 3$) to $\approx 25\%$ ($q = 10$). This indicates that the decreasing trend of ξ_0 with increasing s is maintained by varying q , however the changes are relatively small.

In conclusion, decreased correlation length is a desired

property of the network as it limits the extent of the effect of a perturbation at a given node. According to our analysis, this can be achieved with a line load minimization scheme.

E. Degree Distribution

We proceed to quantify some topological indicators to describe the resulting networks for different s . First we calculate the degree distribution, which fits an exponential function and is insensitive to the value of s . Figure 6(a) shows the degree distribution of networks constructed with $s = 0$ (black), $s = 0.5$ (red), and $s = 1$ (blue) with three different values of r . This type of distribution of power grid connectivity has been reported in

[22], where they considered the growth model in which nodes are placed spatially according to a two-dimensional Poisson point process with constant density and connect to the closest r nodes (i.e., our model with $s = 0$ and $f(x, y) = 1$). Using a mean-field approach, the authors showed that the degree distribution of the resulting network has an exponential tail with exponent $\log[r/(1+r)]$. Remarkably, this theoretical estimate [dashed line in Fig. 6(a)], valid in principle only for $s = 0$, describes well the degree distributions obtained from our model with $s = 0.5$ and $s = 1$ as well. This can be understood by the empirical observation that when a node connects to the network, the choice of which r nodes it connects to has very little correlation with the degree of these nodes as can be verified in Fig. 6(b). For this figure, we perform one realization of network growth, storing at each growing step the quartile at which the degree of the r connected nodes belong to. As seen in the Figure, the distribution of the quartiles are quite uniform, indicating the lack of correlation between the connected nodes and their degree.

Now we show that, using this assumption, the degree distribution is exponential with exponent $\log[r/(1+r)]$ even in the case that nodes are placed according to a non-uniform density $f(x, y)$. Let $n(x, y, k, t)$ be the density of nodes with degree k at position (x, y) at time t , and consider how the number of nodes of degree k in a small region S with area ΔA around (x, y) is expected to change in one time step

$$\begin{aligned} n(x, y, k, t+1)\Delta A - n(x, y, k, t)\Delta A = & \quad (13) \\ n(x, y, k-1, t)\Delta Au & \\ - n(x, y, k, t)\Delta Au, & \end{aligned}$$

where

$$u = \frac{f(x, y)\Delta Ar}{\sum_{k=r}^N n(x, y, k, t)\Delta A}, \quad (14)$$

accounts for the probability that the added node is in the region S [$f(x, y)\Delta A$], and the probability that it connects to a given node, obtained from the ratio of links established to the total number of nodes in S [$r/\sum_{k=r}^N n(x, y, k, t)\Delta A$]. Simplifying, and approximating $n(x, y, k, t+1) - n(x, y, k, t) \approx dn(x, y, k, t)/dt$, we obtain the rate equation

$$\frac{dn(x, y, k, t)}{dt} = \frac{f(x, y)r}{n(x, y, t)}[n(x, y, k-1, t) - n(x, y, k, t)], \quad (15)$$

where $n(x, y, t) = \sum_{k=r}^N n(x, y, k, t)$. As $t \rightarrow \infty$, we look for a stationary solution of the form

$$n(x, y, k, t) = \bar{n}(x, y, k)t, \quad (16)$$

$$n(x, y, t) = f(x, y)t. \quad (17)$$

Inserting this Ansatz in Eq. (15) and simplifying, we obtain

$$\bar{n}(x, y, k) = \frac{r}{1+r}\bar{n}(x, y, k-1), \quad (18)$$

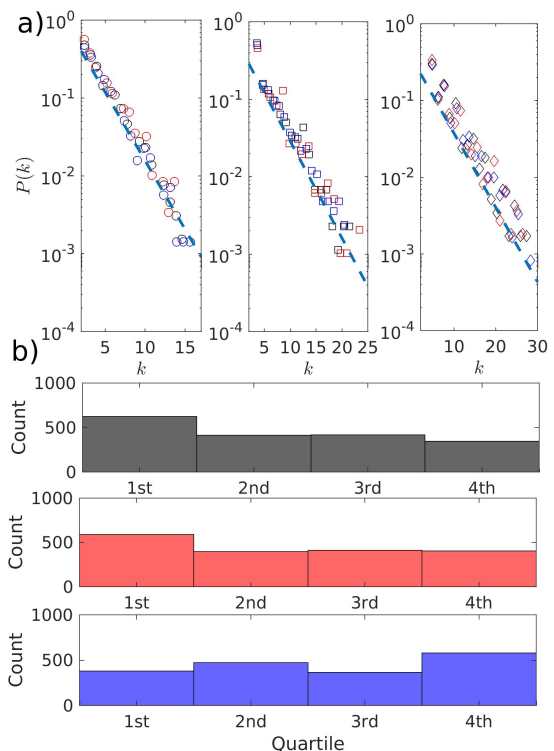


FIG. 6: a) degree distribution of $N = 1000$ networks constructed using our model using $r = 2$ (left), $r = 3$ (middle), and $r = 4$ (right) for $s = 0.0$ (black), $s = 0.5$ (red), and $s = 1.0$ (blue). b): quartile to which the degree of the nodes that new nodes connect to belongs to for $s = 0.0$ (black), $s = 0.5$ (red), and $s = 1.0$ (blue).

so that the limiting distribution \bar{n} is exponential

$$\bar{n}(x, y, k) = \bar{n}(x, y, r)e^{\ln(\frac{r}{1+r})(k-r)}. \quad (19)$$

F. Other topological indicators

Although the degree distribution of the generated networks is insensitive to s , other topological properties are affected by the choice of s . We computed other topological measures that characterize the generated power grids, namely the average betweenness centrality of the network (b), the average clustering coefficient (c), and the characteristic path length (l), defined below:

$$b = \frac{1}{N} \sum_i \sum_{s, t \neq i} \frac{n_{st}(i)}{N_{st}} \quad (20)$$

$$c = \frac{1}{N} \sum_i \frac{T_i}{\mathcal{J}} \quad (21)$$

$$l = \frac{1}{N(N-1)} \sum_{i, j} D_{ij} \quad (22)$$

$$(23)$$

In Eqs. (20)-(22) n_{st} is the number of shortest paths from nodes s and t that pass through i and N_{st} is the total number shortest paths from s to t . T_i is the number of triangles in which node i is involved and \mathcal{T} is the number of connected triplets in the network. Also, D_{ij} is length of the shortest path between the pair of nodes (i, j) . At this level of description the differences between networks created at different weights s start to emerge.

It has been proposed in [14, 15] that resilient power grids are characterized by topologies with small values of average betweenness. This reflects a reduced criticality of the nodes in the network. The networks in our algorithm have shown a decreasing trend of $\langle b \rangle$ for increasing s [see Fig. 7(a)] for the three considered values of r . This seems to suggest that topological resilience is increased when seeking higher stability of the network. Conversely, the same authors showed that networks with larger clustering coefficient and small characteristic path are indicators of efficient power networks with reduced energy losses. From this perspective, the networks generated with our algorithm tend to improve l with increasing s but decreases clustering coefficient, as seen in Figs. 7(b-c), indicating the need of a trade-off between resilience and effectiveness in our networks. It is worth noticing that while the trends described above are maintained for all the values of r studied, the relative differences between small and large s are much more noticeable at low r . Of course the relative change between the topological indicators at small and large s depends on the chosen value of q , namely the number of first neighbors that the greedy algorithm evaluates before choosing r connections. To check this, we calculate the quantity $Q_{\langle x \rangle}$ defined in Eq. (12), with $\langle x \rangle = \{\langle b \rangle, \langle c \rangle, \langle l \rangle\}$ which is depicted in Fig. 8 by fixing $r = 2$. In this Figure, it is possible to see that increasing the value of q , the relative change between $s = 0$ and $s = 1$ increases for all the indicators, specially the clustering coefficient where it changes from 40% to 80%. Recall that, according to the definition in Eq. (12), a positive value of $Q_{\langle x \rangle}$ is the result of a decreasing trend of the indicator at large s . From this, one can easily see that the clustering coefficient decreases more dramatically at large q . This is not surprising because the clustering coefficient reflects how well connected each node's neighbors are between them. Larger q means that is it likely that neighbors are far apart, and therefore the chances that said neighbors are connected between them are rather low. The results varying q and r seem to point out that considering more candidate nodes to connect to may have considerable effects on the efficiency of the network, as clustering is better achieved with local connections. This preference towards local connectivity (decreased line length) should be however balanced with the dynamical features of the network encompassed by the indicator Δ .

IV. CONCLUDING REMARKS

In this paper we have proposed a greedy algorithm for the growth of power grids, including information of the added length and a readily available indicator of the linear stability of the resulting network. We have found that with a slight increase in the total added line we could obtain a significant improvement of the phase-cohesiveness of the network -a measure of the degree of the synchronized state- and therefore network dynamical robustness.

Next, we studied the effect that the different growing protocols had on the linear stability properties of the system, measured by the critical coupling of the resulting networks and the eigenvalues of the Jacobian matrix. We showed that the critical coupling can be substantially reduced when considering a growing protocol that seeks to minimize Δ .

Other approaches to reduce the critical coupling and improve phase-cohesiveness in Kuramoto complex networks have been proposed from an optimization perspective (see for instance [23–25]). These methods attempt to allocate the different network properties (connectivity, frequency of the oscillators, weight of the edges) which optimizes a desired synchronization measure. In contrast, our algorithm is based on purely local and step-wise measures based on real world constraints such as the spatial location of the element of the network.

The analysis of the linear dynamical features of the system (dynamics around the equilibrium state), led to some surprising effects. For example, the dynamics of the network were virtually unchanged under the different values of s . Not only perturbations are damped at the same rate (an expected behavior from the spectrum of eigenvalues), but also the frequency component of the evolution of the perturbation remained unchanged with different s (an effect that cannot be directly concluded from the eigenvalue expression). Despite the evidence that s does not affect the dynamics of small perturbations, it had a dramatic effect decreasing the resulting critical coupling of the networks, a definitely desired attribute of a power grid. Other approaches to the optimization of network stability properties have been studied before. For instance in [21] the authors used variational equations to find connectivity values that enhanced network dynamics in terms of the real part of the eigenvalues, quantifying the rate at which the system is able to damp perturbations. It should be noticed that, in contrast with the cited reference, we used small values of α leading to complex eigenvalues with identical real part, and therefore a similar type of dynamics in terms of perturbation damping.

The results on intermediate perturbation response showed that the extent to which perturbations are transferred to the network (correlation length) can be decreased by considering an optimization process taking into consideration the value of Δ . Decreasing the correlation is a highly desired property which might mitigate cascading failures, a well known catastrophic effect in power grids [26, 27].

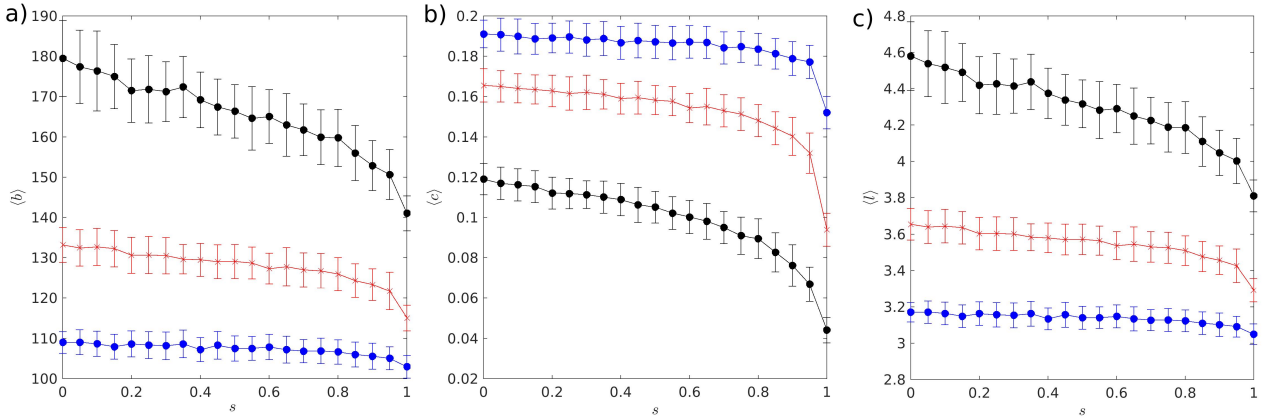


FIG. 7: Topological Indicators: Ensemble average of (a) betweenness centrality, (b) clustering coefficient, and (c) characteristic path length as a function of s . In all panels three values of r were used, namely $r = 2$ (black), $r = 3$ (red) and $r = 4$ (blue). For each value of s , 100 realizations of the algorithm were made with $N_{seed} = 6$ and $N = 100$. Error bars denote the standard deviation across realizations.

After, we showed that tuning the relative importance of the added line vs the dynamical stability of the network has little to no effect in the degree distribution of the resulting network. Indeed the networks generated with the algorithm have all an exponential degree distribution, as has been reported in the literature for several real-world power grids [22, 28–32]. This is an important characteristic, as the resulting grid remains a single-scaled network, avoiding the presence of hubs which heavily undermine network stability.

Finally we analyzed the effect of the growing protocol on other topological features of the network which are

also signatures of network efficiency and resiliency that fall out of the two target variables minimized by the algorithm. In particular, we saw that these two characteristics compete with each other when tuning the parameter s . This result advocates for more complex expressions in the cost function which may account for these features as performed in [15]. However it shall be noticed that our proposal contains the minimal ingredients that capture the two important elements to account for in optimizing power grids, namely topology and dynamics.

Acknowledgments

Damien Beecroft was supported by the Undergraduate Research Opportunities Program at the University of Colorado at Boulder.

Appendix: Stochastic model for node addition

In this Appendix we present a toy model that shows that the effects of the greedy optimization algorithm can be explained from local stochastic considerations. For simplicity, here we use a uniform Poisson process with density λ for the placement of added nodes, i.e., we set $f(x, y) = \lambda$, where $\lambda = 1/\int_M dx dy$.

We start with 2 nodes at time $t = 0$ and assume the initial angle difference $\delta_1 = \theta_1 - \theta_2$ is sampled from a Gaussian distribution with mean σ . The value of σ depends on the value of K used: larger values of K correspond to smaller σ . At time $t = 0$ the line length is $L(0) = 0$, the stability parameter is $\Delta(0) = |\theta_1 - \theta_2|$, and the set of angle differences is $\mathcal{D}(0) = \{\delta_1\}$.

The model then proceeds recursively as follows: at time $t = 0, 1, 2, 3, \dots$, when we already have a set of $n = 1 + rt$ angle differences $\mathcal{D}(t) = \{\delta_1, \delta_2, \dots, \delta_n\}$,

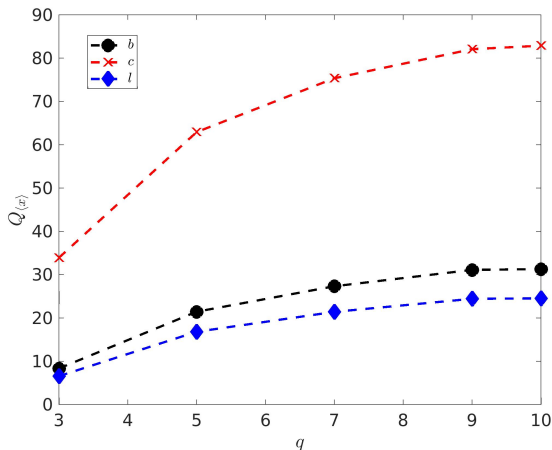


FIG. 8: Relative change between average topological indicators obtained at $s = 0$ and $s = 1$ expressed as a percentage. For this figure, a fixed value of $r = 2$ was set, and then the relative difference between the topological indicator obtained at $s = 0$ and $s = 1$ is expressed as a percentage for varying q . Symbols as expressed in the legend. Parameters of network generation as in Fig. 7

line length $L(t)$ and stability parameter $\Delta(t)$, we simulate the addition of a new node connected to r existing nodes. We sample the distances x_1, x_2, \dots, x_q from the new node to the q closest nodes from the appropriate random variables that describe the 2-D point Poisson process. For example, the distance x_1 to the closest node when N nodes have been added has density $f(x_1) = 2N\pi\lambda x_1(1 - \lambda\pi x_1^2)^{N-1}$. Similarly, we generate the potential angle differences $\tilde{\delta}_{n+1}, \tilde{\delta}_{n+2}, \dots, \tilde{\delta}_{n+q}$ between the new node and the q potential nodes from a Gaussian distribution with mean σ . Then we let

$\bar{\Delta}_j = \max(|\tilde{\delta}_j|, \Delta(t))$, $L_j = L(t) + x_j$ and choose the r nodes i_1, i_2, \dots, i_r with the smallest cost function $s\bar{\Delta}_j + (1 - s)L_j$. We then update the angle differences set to $\mathcal{D}(t+1) = \{\delta_1, \delta_2, \dots, \delta_n, \tilde{\delta}_{i_1}, \tilde{\delta}_{i_2}, \dots, \tilde{\delta}_{i_r}\}$, the stability parameter to $\Delta(t+1) = \max_{\delta \in \mathcal{D}}\{|\delta|\}$, and the line length to $L(t+1) = L(t) + x_{i_1} + \dots + x_{i_r}$. In Fig. 2 we used $\lambda = 0.4$, $\sigma = 0.5$, and simulated the process until $t = 200$. Each point represents the average of 100 realizations.

-
- [1] J. L. Sawin, F. Sverrisson, J. Rutovitz, S. Dwyer, S. Teske, H. E. Murdock, R. Adib, F. Guerra, L. H. Blanning, V. Hamirwasia, et al., Renewables 2018-Global status report. A comprehensive annual overview of the state of renewable energy. Advancing the global renewable energy transition-Highlights of the REN21 Renewables 2018 Global Status Report in perspective (2018).
- [2] P. S. Georgilakis and N. D. Hatziargyriou, IEEE Transactions on power systems **28**, 3420 (2013).
- [3] L. F. Alberto, F. H. Silva, and N. G. Bretas, in *2001 IEEE Porto Power Tech Proceedings (Cat. No. 01EX502)* (IEEE, 2001), vol. 2, pp. 6–pp.
- [4] P. Varaiya, F. F. Wu, and R.-L. Chen, Proceedings of the IEEE **73**, 1703 (1985).
- [5] T. L. Vu and K. Turitsyn, IEEE Transactions on Automatic Control **62**, 1165 (2016).
- [6] F. Dörfler, M. Chertkov, and F. Bullo, Proceedings of the National Academy of Sciences **110**, 2005 (2013).
- [7] P. J. Menck, J. Heitzig, J. Kurths, and H. J. Schellnhuber, Nature communications **5**, 1 (2014).
- [8] A. E. Motter, S. A. Myers, M. Anghel, and T. Nishikawa, Nature Physics **9**, 191 (2013).
- [9] X. Zhang, C. Ma, and M. Timme, Chaos: An Interdisciplinary Journal of Nonlinear Science **30**, 063111 (2020).
- [10] A. N. Montanari, E. I. Moreira, and L. A. Aguirre, Communications in Nonlinear Science and Numerical Simulation **89**, 105296 (2020).
- [11] P. Schultz, J. Heitzig, and J. Kurths, New Journal of Physics **16**, 125001 (2014).
- [12] M. F. Wolff, P. G. Lind, and P. Maass, Chaos: An Interdisciplinary Journal of Nonlinear Science **28**, 103120 (2018).
- [13] P. Schultz, J. Heitzig, and J. Kurths, The European Physical Journal Special Topics **223**, 2593 (2014).
- [14] G. A. Pagani and M. Aiello, Physica A: Statistical Mechanics and its Applications **449**, 160 (2016).
- [15] L. Cuadra, M. D. Pino, J. C. Nieto-Borge, and S. Salcedo-Sanz, Energies **10**, 1097 (2017).
- [16] A. Fabrikant, E. Koutsoupias, and C. H. Papadimitriou, in *International Colloquium on Automata, Languages, and Programming* (Springer, 2002), pp. 110–122.
- [17] G. Filatrella, A. H. Nielsen, and N. F. Pedersen, The European Physical Journal B **61**, 485 (2008).
- [18] M. Rohden, A. Sorge, D. Witthaut, and M. Timme, Chaos: An Interdisciplinary Journal of Nonlinear Science **24**, 013123 (2014).
- [19] M. Rohden, A. Sorge, M. Timme, and D. Witthaut, Physical review letters **109**, 064101 (2012).
- [20] C. C. Galindo-González, D. Angulo-García, and G. Osorio, New Journal of Physics **22**, 103033 (2020).
- [21] B. Li and K. M. Wong, Physical Review E **95**, 012207 (2017).
- [22] D. Deka, S. Vishwanath, and R. Baldick, IEEE Transactions on Smart Grid **8**, 2794 (2016).
- [23] P. S. Skardal, D. Taylor, and J. Sun, Physical review letters **113**, 144101 (2014).
- [24] P. S. Skardal, D. Taylor, and J. Sun, Chaos: An Interdisciplinary Journal of Nonlinear Science **26**, 094807 (2016).
- [25] M. Fazlyab, F. Dörfler, and V. M. Preciado, Automatica **84**, 181 (2017).
- [26] L. Duenas-Osorio and S. M. Vemuru, Structural safety **31**, 157 (2009).
- [27] P. Hines, K. Balasubramaniam, and E. C. Sanchez, Ieee Potentials **28**, 24 (2009).
- [28] R. Albert, I. Albert, and G. L. Nakarado, Physical review E **69**, 025103 (2004).
- [29] R. V. Solé, M. Rosas-Casals, B. Corominas-Murtra, and S. Valverde, Physical Review E **77**, 026102 (2008).
- [30] P. Crucitti, V. Latora, and M. Marchiori, Physica A: Statistical mechanics and its applications **338**, 92 (2004).
- [31] M. A. S. Monfared, M. Jalili, and Z. Alipour, Physica A: Statistical Mechanics and its Applications **406**, 24 (2014).
- [32] D. H. Kim, D. A. Eisenberg, Y. H. Chun, and J. Park, Physica A: Statistical Mechanics and its Applications **465**, 13 (2017).